Meteorol. Atmos. Phys. 44, 43–61 (1990)

Meteorology and Atmospheric Physics

551.515.5

Department of Meteorology, University of Hawaii, Honolulu, Hawaii, USA

Synoptic Climatology of Transient Tropical Intraseasonal Convection Anomalies: 1975–1985*

B. Wang and **H. Rui**

With 12 Figures

Received June 22, 1989
Revised November 3, 1989

Summary

Pentad mean anomaly maps were used to study the climatology of tropical intraseasonal convection anomaly (TICA) as a dynamic system. One hundred and twenty-two events were identified and classified into three categories: eastward (77), independent northward (27), and westward (18) propagation. The eastward propagation is more active in boreal winter than in summer, while the independent northward propagation, which is not associated with equatorial eastward propagation, occurs in boreal summer from May to October.

The eastward moving TICA exhibits three major paths: 1) eastward along the equator from Africa to the mid-Pacific, 2) first eastward along the equator, then either turning northeast to the northwest Pacific or turning southeast to the southwest Pacific at the maritime continent, and 3) the main anomaly moves eastward along the equator with split center(s) moving northward over the Indian and/or western Pacific Oceans. The equatorial Indian Ocean and the western Pacific intertropical convergence zone are preferred geographic locations for their development, while the maritime continent and central Pacific are regions of dissipation.

Independent northward propagation is confined to the Indian and western Pacific monsoon regions. Its existence suggests that the mechanism responsible for meridional propagation may differ from that for eastward propagation.

The dynamic effect of the equator and the thermodynamic effect of the underlying warm ocean water are basic factors in trapping TICA in the deep tropics, while the annual march of maximum SST (thermal equator) and the monsoon circulation have profound influences on the annual variation and meridional movement of TICA.

* Contribution No. 89–11, Department of Meteorology, University of Hawaii.

1. Introduction

The tropical intraseasonal oscillation is one of the most intensively studied large-scale low-frequency phenomenon in recent years. Pioneering research (Madden and Julian 1971, 1972; Yasunari 1979) used spectral and cross spectral analysis of station data to reveal statistical features in the frequency domain. Correlation maps and empirical orthogonal function (EOF) analyses have been employed to document the propagation and teleconnection pattern from time-space domain using outgoing longwave radiation (OLR) and objectively analyzed wind data (e.g., Lau and Chan, 1985; Weickmann et al., 1985; Lorenc, 1984; Murakami and Nakazawa, 1985). It has been generally recognized that the oscillations are associated with the movement of low-frequency circulation and convection anomalies. We refer to them as tropical intraseasonal convection anomaly (TICA).

From a dynamical viewpoint, it is more meaningful to identify TICAs from relatively raw data and investigate their behaviour event by event. Krishnamurti and Subrahmanyam (1982) and Weickmann et al. (1989) presented examples of case studies. This paper presents a climatological analysis using pentad mean anomaly (PMA) maps. The PMA maps describe variations on multiple temporal and spatial scales and carry signals

of nonlinear evolution due to scale interactions. The identification of an individual event is thus a challenging task. On the other hand, this procedure is particularly useful in developing a synoptic climatology of TICA as a real dynamic system and in revealing fundamental dynamic factors for the climatology.

The basic focus is on the analysis of common behaviors of the TICA in movement, geographic dependence of the development, temporal variations and their relation to environmental setting.The procedures for constructing PMA maps and defining TICA are described in the next section. The syntheses of the individual events are somewhat complicated because of the great diversity of the phenomenon. Nevertheless, models for various types of TICA based on their movement characteristics are proposed in Sections 3 through 5. Sections 6 and 7 discuss the geographic dependence of development and annual variation of the TICA activities, respectively. Discussions on dynamic factors which may contribute to the synoptic climatology are presented in the last section.

2. Pentad Mean Anomaly Map and Intraseasonal Convection Anomalies

Data used are ten-year OLR (1975–1985, no 1978) from the National Oceanic and Atmospheric Administration (NOAA) and 7-year (1979–1985) wind data from the European Centre for Medium-Range Weather Forecasts. For computational efficiency, a nine-point weighted average is applied to reduce the horizontal resolution to $5° \times 5°$ grids (Rui and Wang, 1989).

The temporal variation of daily data at any fixed grid is decomposed into four components: the interannual, annual, intraseasonal, and synoptic variation. The climatological annual cycle is defined as the sum of the overall mean and the first three Fourier harmonics of the climatological mean daily time series. Subtracting the annual cycle from original daily data yields a daily anomaly time series from which monthly mean anomalies are calculated. The interannual variation is estimated by a weighted three-month running mean (weights are 1:2:1). To focus on intraseasonal variation, we first remove the interannual component from daily anomalies and then compute non-overlapping five-day averages or PMA series.

The PMA maps cover the global tropics and subtropics between 40 °N and 40 °S. In producing PMA maps, spatial smoothing is applied by weighted average in an area of 15 degree latitude by 35 degree longitude. PMA maps describe variations on broad temporal scales ranging from about ten days to three months, and on spatial scales of wavenumber one to six.

Next, we define an TICA in PMA OLR maps as an OLR low system that satisfies three objective criteria: 1) Its life span must be longer than four pentads. 2) During the entire life span, its zonal dimension must exceed 30 degrees longitude, and its central OLR anomaly must be lower than $-15\,W\,m^{-2}$. 3) At its strongest stage of evolution, the zonal dimension must be larger than 50 degrees longitude and the OLR anomaly must be lower than $-25\,W\,m^{-2}$. These TICAs represent large-scale, long-lasting convective anomalies. The evolutionary process from inception to dissipation is referred to as a TICA event.

The following information was tabulated for each event: 1) The tag number indicating the year and months during which the TICA reaches its maximum intensity (minimum OLR anomaly), 2) the longitude and latitude of the TICA center[1], and 3) the central intensity at each pentad. For convenience, the intensity is expressed in terms of the number of negative OLR contours enclosing the center. Thus the numbers 1, 2, 3, ..., represent values of central OLR which are approximately -10, -20, -30, ..., $W\,m^{-2}$, respectively.

Characteristic parameters can then be derived from these tabulated data. They include the life span, total zonal displacement, mean propagation speed, and the intensity index which is defined as the sum of the central intensity at each pentad for the entire period of the event. Each event is classified according to an intensity index: strong (more than 26), moderate (18–26), and weak (less than 18).

The TICA movement as seen in the PMA maps has more complicated patterns in comparison to maps derived from cross-spectral, correlative, or EOF analyses. TICA propagations can be clas-

[1] The center usually corresponds to the minimum in the OLR anomaly field. In a few cases, either multiple minima or irregular geometry for the negative anomaly area are apparent. In these cases, the geometric center is chosen to be the TICA center.

sified into three categories: eastward, independent northward, and westward. Each in turn will be discussed in next three sections.

3. Eastward Moving TICAs

Seventy-seven eastward propagating TICA events have been identified among which 72 occurred in the Eastern Hemisphere. These events do not include those for which the total eastward displacement is less than 50 degrees longitude and the life span is shorter than four pentads. Three types of eastward propagating TICAs are recognized according to the paths of their movement.

The first type (32 cases) is an equatorial trapped mode whose center is confined to a narrow equatorial belt between 15 °N and 15 °S. We refer to this type as equatorial eastward propagating (EE) mode. In Fig. 1 a large area of negative OLR anomaly (convection) first becomes organized over the region from the equatorial Atlantic to Africa during January 21–25 (pentad 1). Five days later (pentad 2), the convection anomaly quickly moves eastward by about 50 degrees longitude with two separate centers located at equatorial Africa and the eastern Indian Ocean, respectively. In the next two pentads, there is a rapid intensification. By pentad 4 (February 5–9), the central OLR anomaly drops below $-65\,W\,m^{-2}$. A well-established dipole structure (Lau and Chan, 1985) forms with convection centered in the Indian Ocean and a dry region covering western Pacific. Note that during this developing stage the eastward movement is not significant. The mature system then moves systematically eastward at a speed of about 4 degrees longitude per day. The dipole structure at pentad 8 (February 25. March 1) is nearly opposite to that of pentad 4. The eastward movement continues until pentad 10 (March 7–11) when the convection anomaly reaches the date line. At this phase, the convection anomaly moves away from the equatorial region toward North America and the southeast Pacific, respectively. Examination of daily satellite images reveals that these negative OLR anomalies in the northeast Pacific may be related to cloudiness fluctuations in the subtropical jet in this region rather than convective activities. The last two pentad mean maps show a rapid collapse of convection leading to termination of the event. The entire evolution bears close similarities to the composite life cycle of the strong eastward-travelling intraseasonal convection anomalies as described in detail by Rui and Wang (1989).

The composite TICA displays a highly coherent dynamic structure in convection, winds, divergent and vertical motion fields. Shown in Fig. 2 are PMA maps of differential divergence between 200 and 850 mb which is a two-level model estimate of the large-scale upward motion at midtroposphere. Overall, there is a high correlation between negative (positive) OLR and rising (sinking) motion in the equatorial region between 15 °S and 15 °N, although the latter tends to have a smaller horizontal scale. The association of negative OLR anomalies and upward motions is particularly evident after the mature phase, that is, from pentad 5 to pentad 11. The general dynamic consistency between OLR and the divergent circulation adds confidence to the above analyses.

The second type of eastward moving TICA (25 cases) follows initially a similar track as the EE mode over Africa and the Indian Ocean but turns either northeast or southeast (or in a few cases, splits into two separate centers with one moving northeast and the other southeast) when passing through the maritime continent. This type of TICA will be referred to as a N(S)E mode. Figure 3 depicts a N(S)E event occurring in late March and April 1985 and lasting for eight pentads. During the first four pentads, a TICA develops in the equatorial African region, it then moves slowly eastward to the equatorial Indian Ocean (75 °E, 0°) where, it rapidly intensifies as indicated by the minimum OLR decreasing from $-30\,W\,m^{-2}$ to $-50\,W\,m^{-2}$ (pentad 4). At pentad 5 (April 11–15), the convection center reaches 100 °E where it begins to split. By the next pentad two distinct centers are evident, one at 130 °E, 8 °N, and the other over western Australia (130 °E, 23 °S). The northern center moves east-northeastward for three pentads, then dissipates northwest of Hawaii, while the southern center moves southeastward for only one pentad before dissipating near New Zealand. Among the total 25 N(S)E events: 13 propagate northeast, 10 move southeast, and 2 split toward both Northern and Southern Hemisphere subtropics.

The third type (20 cases) which is referred to as an EN mode is characterized by a combination of a major equatorial eastward movement with northward movement(s) over the Indian and/or

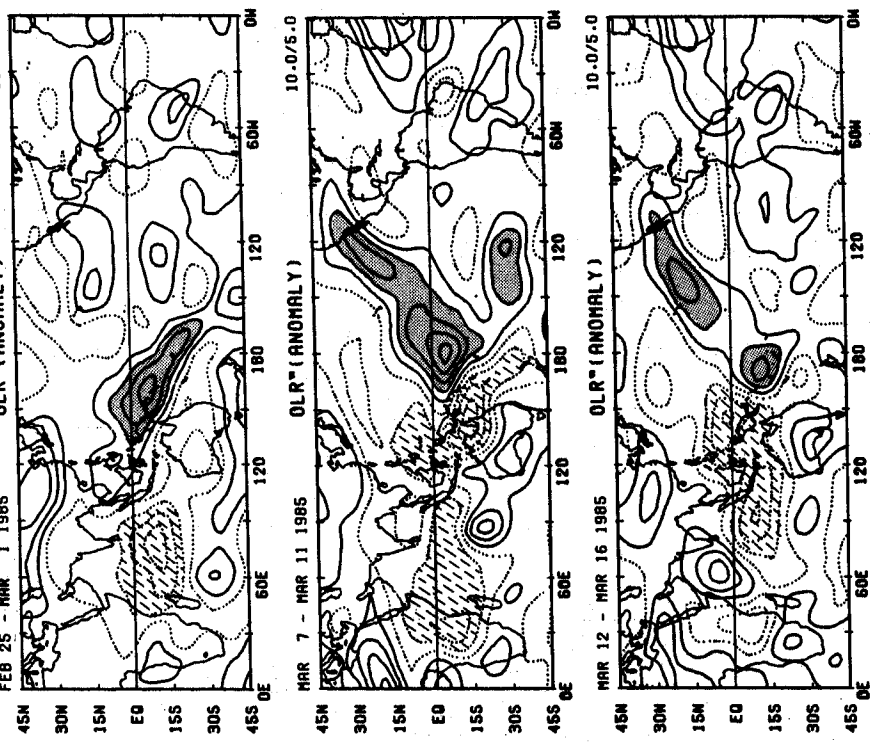

Fig. 1. A sequence of OLR PMA maps for an equatorial eastward moving TICA event. Solid (dotted) contours represent negative (positive) values equal or less (greater) than $-5(5)$ W m^{-2}. Contour interval is 10 W m^{-2}

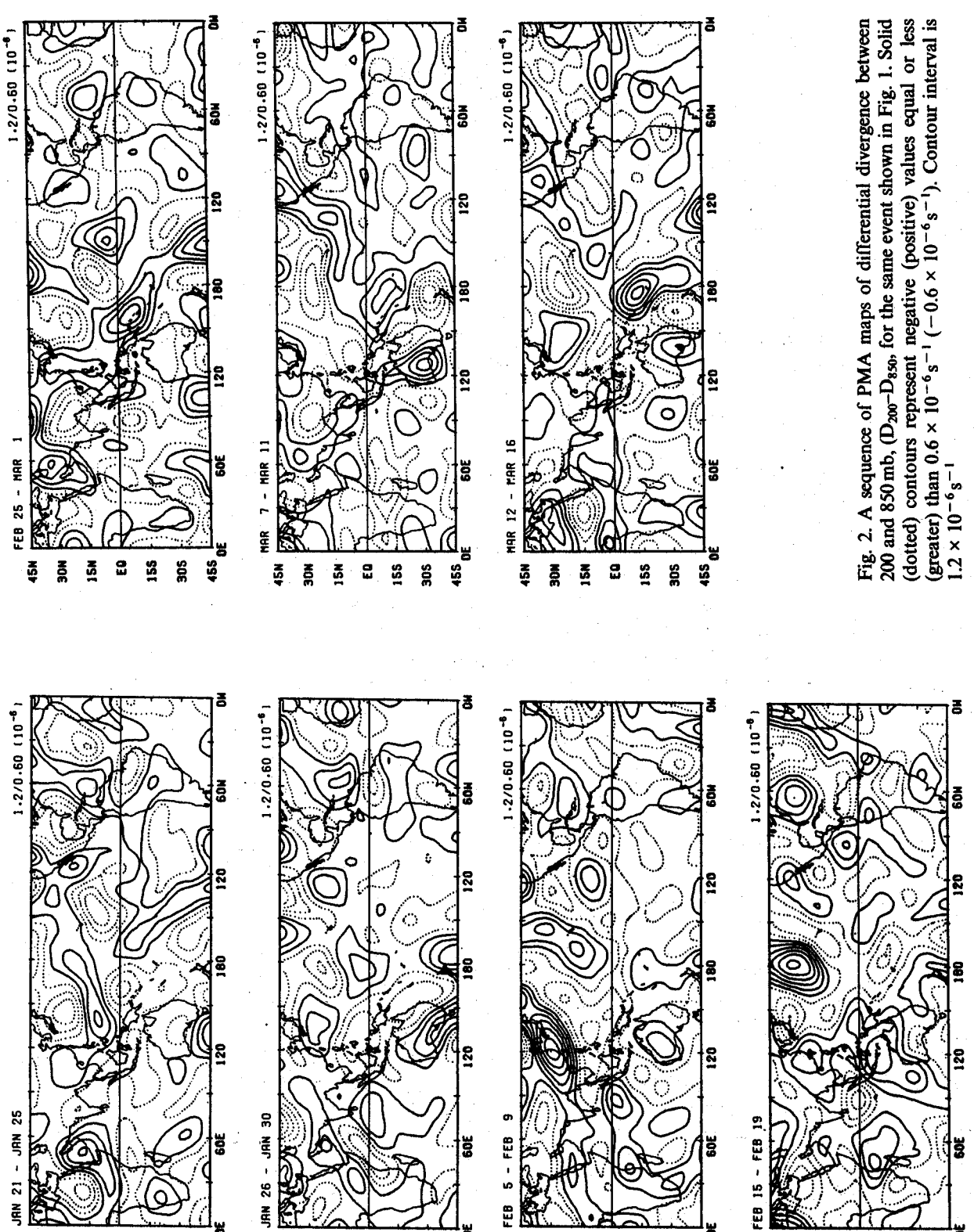

Fig. 2. A sequence of PMA maps of differential divergence between 200 and 850 mb, (D_{200}–D_{850}), for the same event shown in Fig. 1. Solid (dotted) contours represent negative (positive) values equal or less (greater) than $0.6 \times 10^{-6} s^{-1}$ ($-0.6 \times 10^{-6} s^{-1}$). Contour interval is $1.2 \times 10^{-6} s^{-1}$

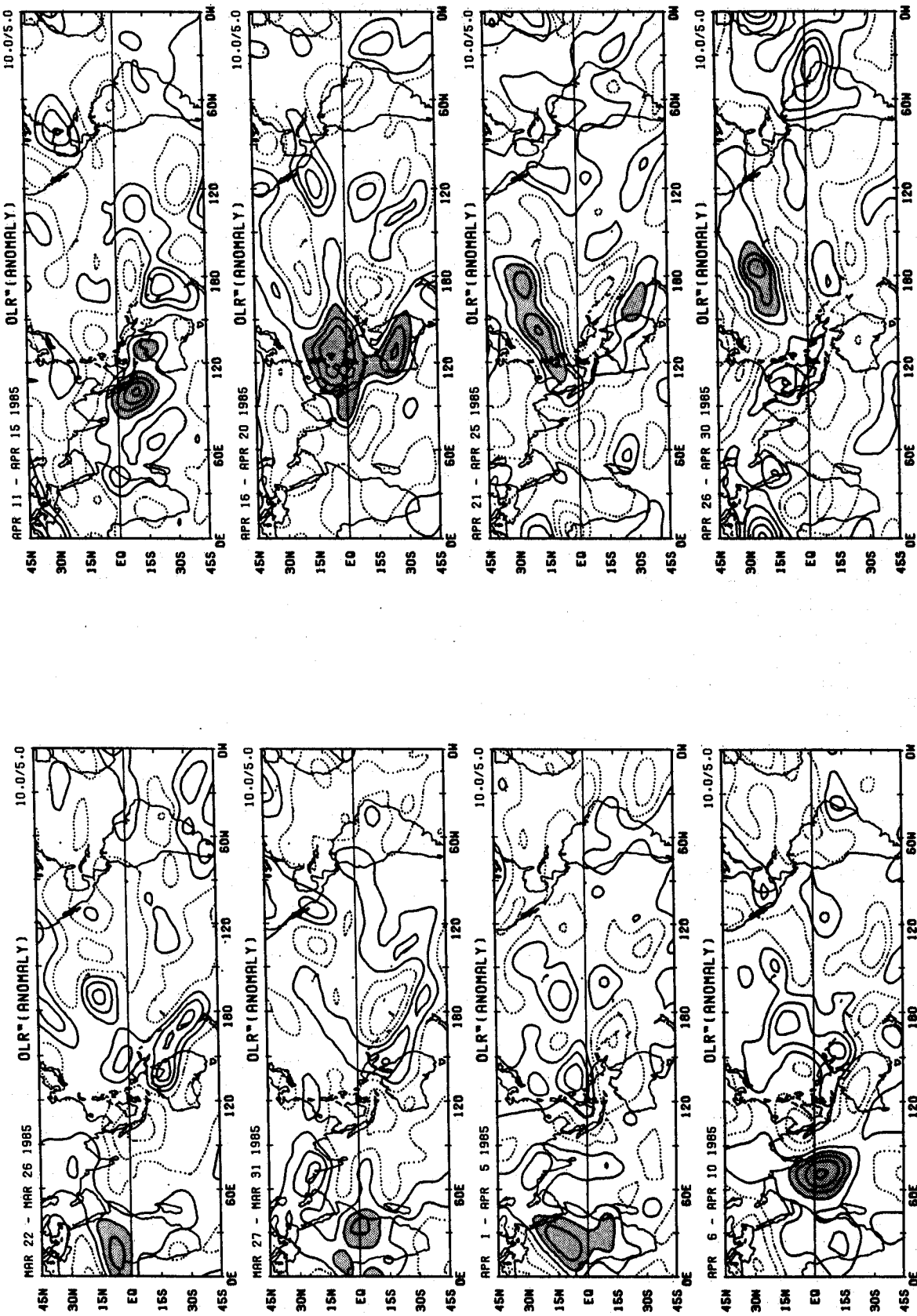

Fig. 3. As in Fig. 1 except for an eastward moving event of N(S)E mode (see text for explanation) during March-April 1985

Fig. 4. As in Fig. 1 except for an eastward moving event of E-N mode (see text for explanation) occurring during August-September 1976

western Pacific monsoon regions. A typical example is presented in Fig. 4. A well-defined convection anomaly is noticeable during August 19–23, 1976 (pentad 2) over the central equatorial Indian Ocean, it appears to have originated over equatorial Africa during the preceding pentad. In the next five days the convection anomaly expands in the meridional direction, while propagating to the eastern Indian Ocean with a minimum south of Sri Lanka (80 °E, 6 °N). By pentad 4 (August 29 – September 2), the anomaly splits into two nearly distinct parts with one moving eastward along the equator to the maritime continent and the other northward to south India (80 °E, 14 °N). The central equatorial Indian Ocean becomes dry. By pentad 5 (September 3–7), the northward moving convection anomaly is located over the northern Arabian Sea with a significant decrease in its intensity and size. On the other hand, the equatorial convection anomaly continues its eastward migration to the western Pacific (150 °E, 0°). The anomaly approaches the date line at the sixth pentad (September 8–12) where it splits once again with one component heading north-northwestward in the western Pacific (155 °E, 15 °N) and the other moving eastward to the central Pacific (150 °W, 5 °E).

The frequency of occurrence for TICA centers in each 2° × 2° box is shown in Fig. 5 for EE mode (a), N(S)E mode (b), and EN mode (c). The axes of maximum frequency are representative of the prevailing track tendency. The EE modes usually appear in a narrow equatorial belt between 30 °E and 150 °W. Their maxima are located on the both sides of the maritime continent between 90 °E and 150 °E (Fig. 5 a). The centers of all N(S)E mode are confined to the equatorial belt west of 100 °E over the Indian Ocean, with branches extending poleward to the subtropics of both hemispheres east of 100 °E. The northern branch of high frequency of occurrence extends from the maritime continent, across south China and the Philippine Sea, all the way to the date line at 20 °N, whereas the southern branch runs across northern Australia, to 150 °W, 15 °S (Fig. 5 b). The EN mode has two maximum frequency of occurrence: one over the central Indian Ocean (85 °E, 0°), and the other in the equatorial western Pacific (145 °E, 4 °N). From these two centers bands of relatively high frequency of occurrence extend to norther India and the south of Japan, respectively. An elongated belt of high frequency of occurrence near the equator indicates a major branch of eastward movement along the equator (Fig. 5 c).

Figure 5 d synthesizes all three types of eastward moving TICAs which occur in the Eastern Hemisphere (72 cases). The thick lines with arrows highlight the major mean paths for the three types of eastward propagation. The maximum frequency is located at 82 °E, 0°. A secondary maximum appears in the western end of the equatorial Pacific between 120 °E and 150 °E. It is noteworthy that the eastward travelling TICAs not only occur near the equator of Eastern Hemisphere, but are also found in the subtropical monsoon regions (India, southeast Asia, western Pacific, and northern Australia). This is indicative of the influence of monsoonal flows on TICA's activities.

Recall that all eastward moving TICAs are categorized according to their intensity, i.e., strong, moderate, or weak. In Table 1 the number of events, the average total eastward displacement, maximum intensity, duration, and zonal propagation speed for each class of eastward moving events are presented. Although some eastward moving TICAs display meridional movement, the zonal propagation speed and longitude displacement here express only the zonal components of the rate of propagation and of the total displacement, respectively.

4. Independent Northward-Moving TICAs

To detect meridional movement, we constructed time-latitude diagrams of pentad mean OLR anomalies zonally averaged along three longitude bands (67.5°–92.5 °E, 97.5°–122.5 °E, and 127.5°–152.5 °E) from 40 °S to 40 °N (figures are not shown). Southward movement is rare and primarily confined to the maritime continent-northern Australia region. Most southward propagation represents meridional components of the SE mode discussed in the previous section. The northward movement from the equator to the Northern Hemisphere subtropics, however, is more clearly defined. Most events occur in two sectors: the Indian Ocean (70°–90 °E, 0°–25 °N) and the western Pacific (130°–150 °E, 0°–30 °N) monsoon regions. The northward propagating events display smaller horizontal scales on PMA maps and shorter durations compared with those moving predominantly eastward. Northward moving

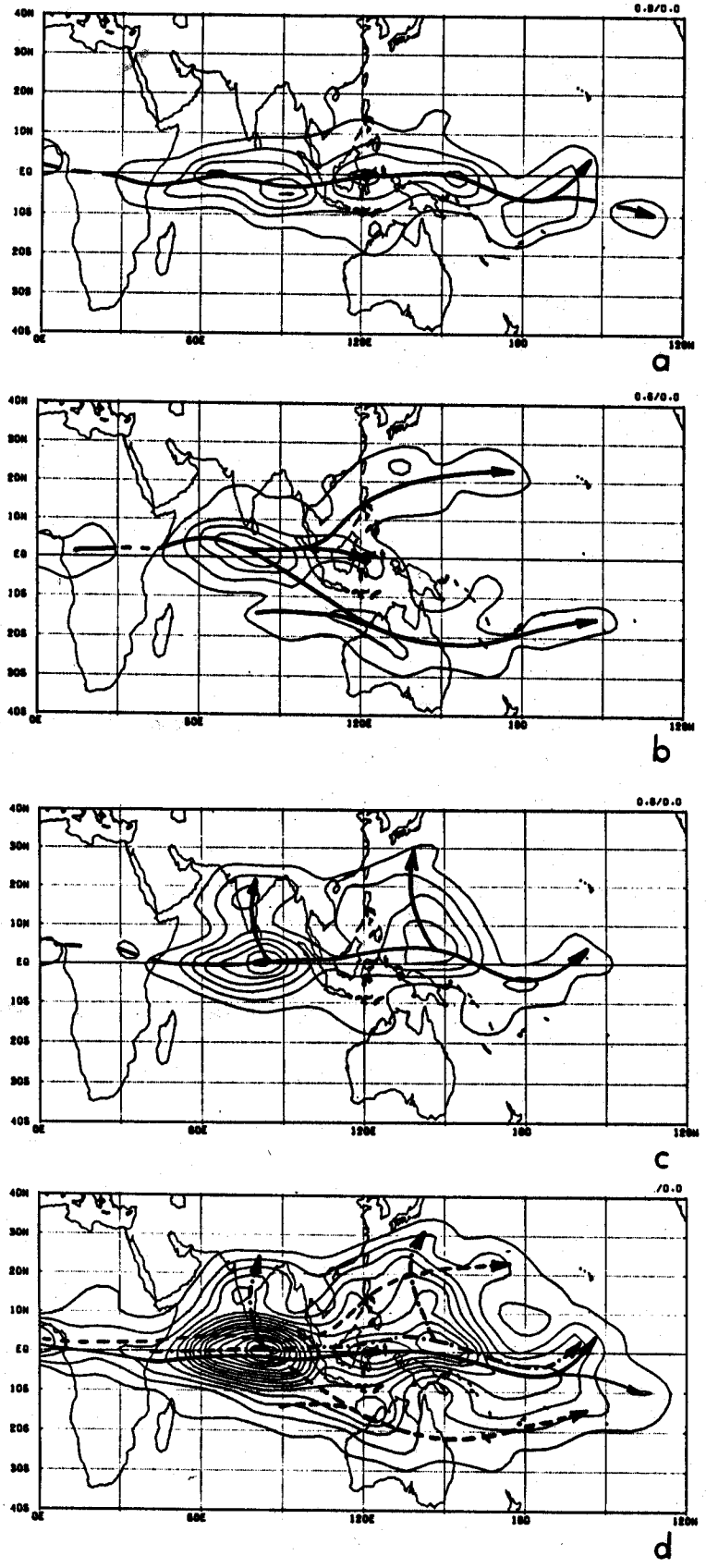

Fig. 5. Contour plot of total number of occurrence of centers for (a) EE mode; (b) N(S)E mode; (c) EN mode; and (d) all eastward propagating modes (the sum of (a), (b), and (c)) in each 2° × 2° box for a ten-year period (1975–1985). The contour interval is 0.8 except in (b) which is 0.6. The thick solid, dashed, and dark dotted lines with arrows in (d) indicate the central paths for EE, N(S)E, and EN modes, respectively. For an explanation of EE, N(S)E, and EN modes, refer to the text

Table 1. *Statistics for the Eastward Moving TICAs*

Intensity classification	Strong	Moderate	Weak	Total
Number of cases (events)	22	28	27	77
Mean total eastward displacement (longitude)	148	143	102	130
Mean minimum OLR ($W m^{-2}$)	−36	−36	−32	−37
Mean duration (pentad)	9.8	7.4	5.2	7.2
Mean propagation speed ($m s^{-2}$)	4.2	5.2	5.2	4.9

events were identified from ten years of OLR maps. The number of cases occurring in the Indian monsoon region is about the same as those in the western Pacific monsoon region.

There are two distinguishable types of northward moving events. The first type is an independent northward propagation without an association with zonal propagation. A convection "burst" originates near the equator, intensifies, propagates northward, and finally dissipates in the subtropics. The second type, on the other hand, is intimately associated with major equatorial zonal propagation. It represents the meridional components of the EN mode discussed in the previous section. It has been suggested that the northward propagation in the Indian monsoon region is an integral part or a meridional component of the equatorial eastward moving circulation anomalies (e.g., Julian and Madden, 1981; and others). We found that this is only analogous to the NE modes or the second type of northward movement.

Dynamically, it is more interesting to examine independent northward moving events. One such example occurring over the Indian monsoon region is presented in Fig. 6. During the initial stage (pentad 1, September 18–22, 1984), there is a weak convection anomaly region located at the central-eastern equatorial Indian Ocean, while the India and south Asia are dry. In the subsequent two pentads, this convective anomaly region rapidly intensifies and expands in size. The central OLR value decreases from $-20 W m^{-2}$ to $-50 W m^{-2}$. Meanwhile, its central location shifts north-northwestward from south of the equator to the south end of India. From pentad 4 on, this convective anomaly region turns northeastward, crosses the Bay of Bengal and finally dies out in southeast Asia. At the same time the central Indian Ocean experienced its dry phase. During the entire six-pentad period, there is no signal of eastward propagation along the equatorial belt. The mid-tropospheric rising motion anomaly as depicted by the differential divergence field (not shown), accompanies the convection anomaly and migrates systematically from south of the equator around 85 °E, 3 °S to north of the Bay of Bengal. The agreement between positive OLR anomalies and sinking motion region is also remarkable.

Another independent northward moving event occurring over the western Pacific monsoon region is shown in Fig. 7. During July 30 through August 3, 1984 (pentad 1), a vast area of the tropical western Pacific is occupied by a giant OLR low with a zonal scale in excess of 70 degrees longitude, whereas the eastern equatorial Indian Ocean is dry with a maximum positive OLR anomaly greater than $25 W m^{-2}$. At pentad 2, the OLR anomaly over the western Pacific breaks into two large-scale OLR lows; one moves into the central Pacific and rapidly decays, and the other propagates northward to south China and the Philippine Sea with increasing convective activity. From pentad 2 to 5, there is a slow but rather steady north-northeastward drift over the western Pacific monsoon region along 130 °E. During this process, the convection anomaly intensifies, reaching its peak stage at pentad 4 (August 14–18) with an OLR anomaly below $-45 W m^{-2}$ located north of the Philippine Sea, while the equatorial western Pacific-maritime continent region changes into a dry regime. Subsequently, the convection anomaly decays south of Japan. This case also displays a coherent divergent wind field structure (not shown).

All independent northward moving events (27) appear in boreal summer from May to October. There are two formation regions: one is the equatorial Indian Ocean and the other is the equatorial western Pacific (Fig. 8). Over the Indian monsoon region the major track of northward displacement

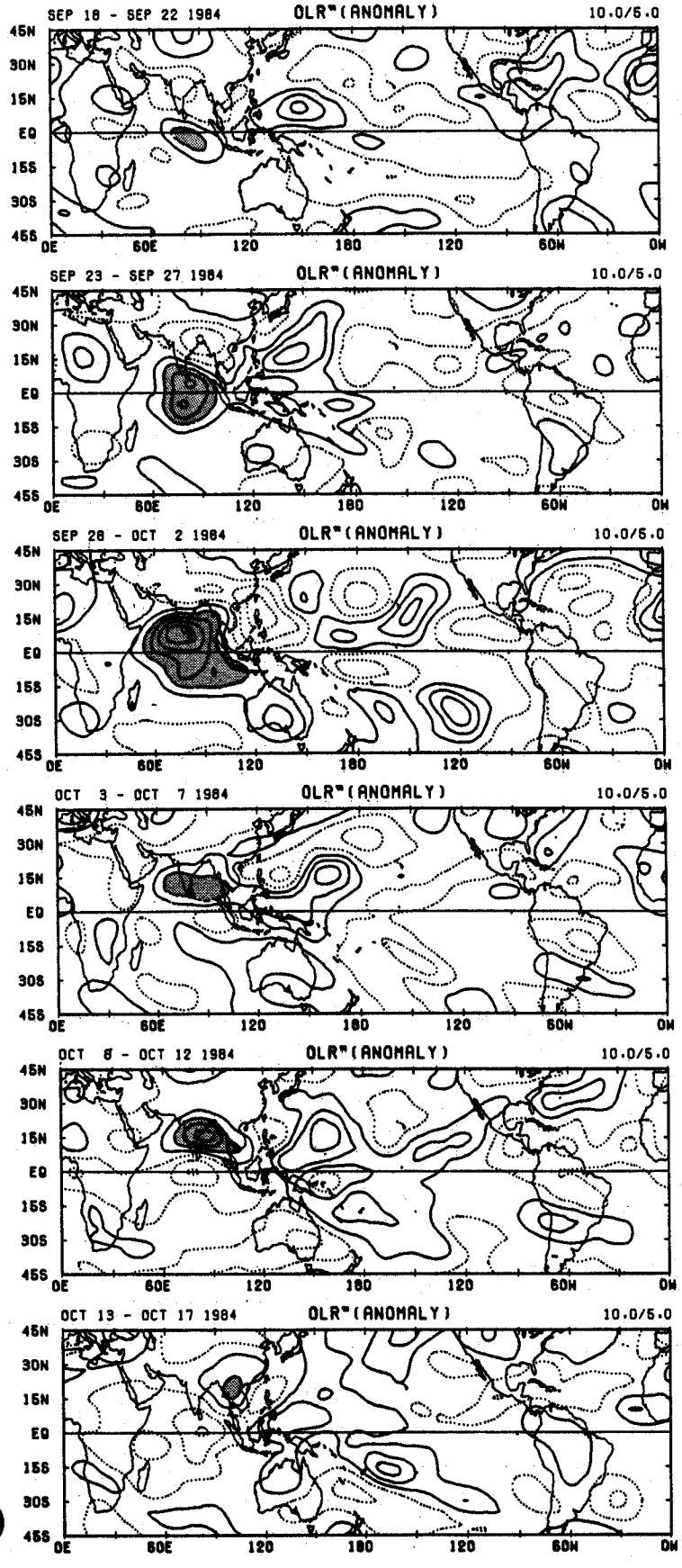

Fig. 6. As in Fig. 1 except for an independent northward moving event over the Indian monsoon region occurring during September-October 1984

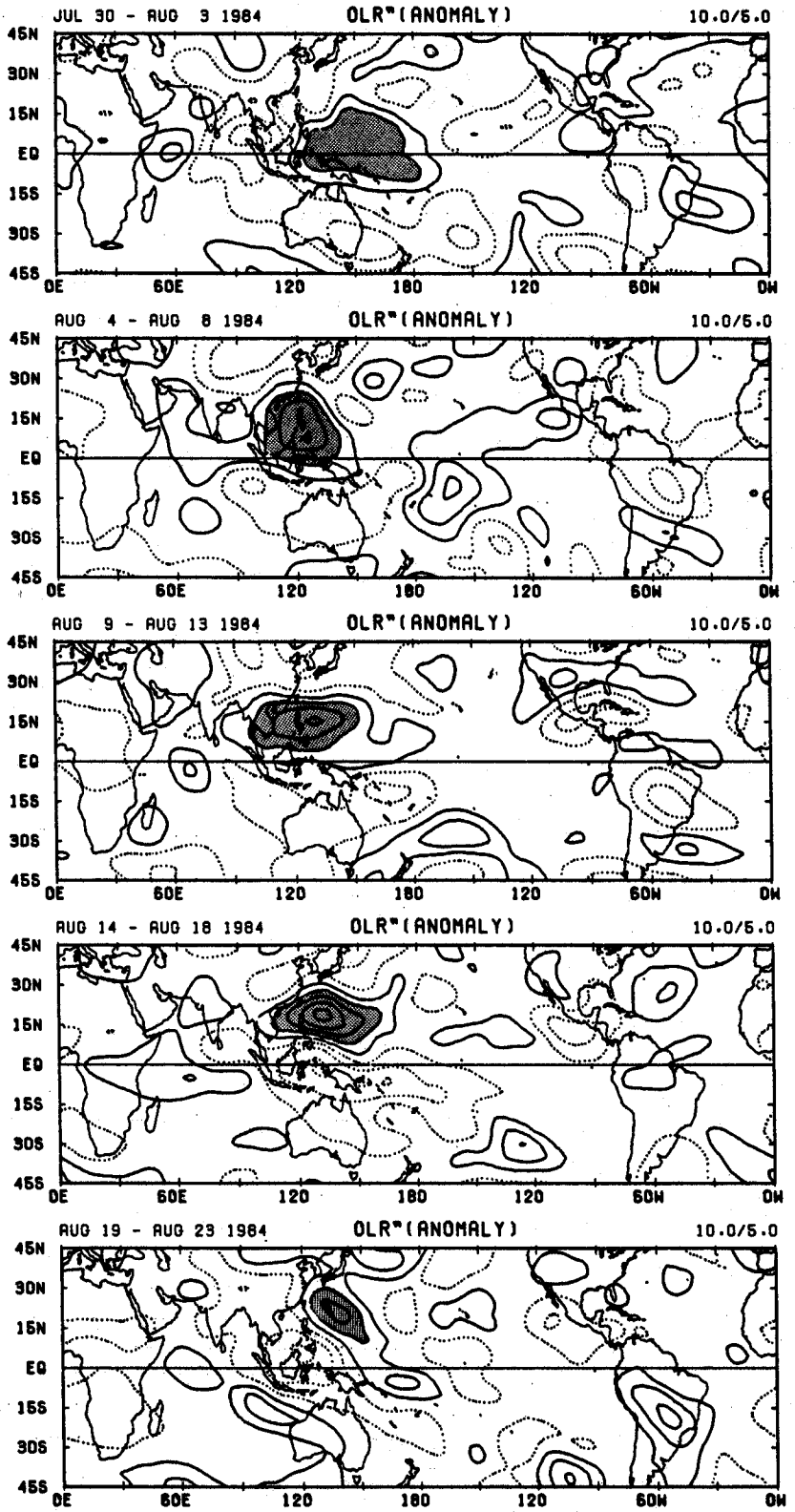

Fig. 7. As in Fig. 6 except for an independent northward moving event over the northwestern Pacific Ocean occurring during August 1984

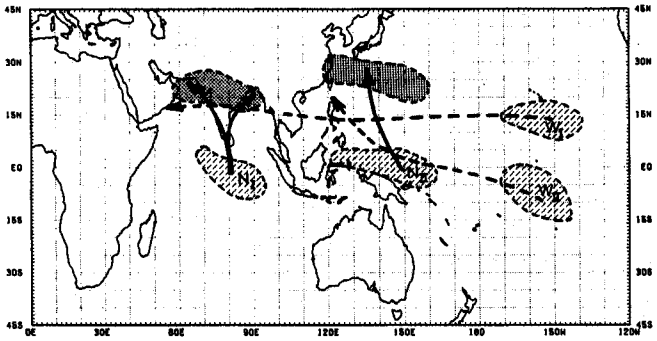

Fig. 8. Schematic diagram illustrating the mean paths for the independent northward moving TICAs over the Indian Ocean (NI) and over the western Pacific (NP) regions (thick solid line) and for westward moving (W_I and W_{II}) TICAs (thick dashed). The hatching (mesh) areas indicate formation (dissipation) regions

splits over southern India with branches directed to the Bay of Bengal and the Arabian Sea, respectively. The underlying warm ocean surface and associated large surface heat fluxes may be a factor in determining the central track of these TICAs. Others have noticed the close association between the northward migration of the TICA and the onset and/or wet spell of the Indian monsoon (Krishnamurti and Subrahmanyam, 1982; Murakami et al., 1986). Over the western Pacific the TICA's central track tends to head north-northwestward and to dissipate south of Japan (Fig. 8).

One may question whether the northward movement of TICAs is dominated by individual tropical storms or typhoons. Checking the annual typhoon report published by the Joint Typhoon Warning Center at Guam for all independent northward moving events, it was found that some events indeed involved multi-tropical storm motions. There is no doubt that long-lasting synoptic-scale tropical storms make significant contributions to the low-frequency convective anomalies. Yet, the TICA depicted by the PMA map does not reflect any individual typhoon, rather it represents the collective activities of many synoptic or subsynoptic tropical convective systems, such as tropical storms, depressions, and cloud clusters, etc. For instance, the event shown in Fig. 7 lasts five pentads, during which one typhoon (TY HOLLY, August 16–22), two tropical storms (TS TREAD, August 5–8; and TS GERALD, August 16–20), and one tropical depression (TD 09W, August 11–15) are involved. None of these tropical systems could dominate the TICA's motion; they only contribute a small or moderate portion to the movement of the large-scale TICA. While it is possible that cumulus ensembles are directly organized by tropical cloud cluster scale systems, the latter is in turn modulated by the moisture convergence provided by very large-scale low-frequency disturbances. In this sense, the TICA should be viewed as an ensemble of cloud cluster or synoptic scale systems.

Table 2 shows the statistics of the independent northward moving events. The mean total northward displacement is about 22 degrees latitude and the mean duration is approximately four pentads. The mean phase speed (about one degree per day) appears to agree with the results obtained in previous studies (e.g., Krishnamurti et al., 1985).

5. Westward Propagation

In addition to the aforementioned eastward propagation and independent northward propagation in the summer monsoon region, we also notice some relatively weak westward moving TICAs. Eighteen westward moving events with a total longitudinal displacement longer than 60 degrees and a duration longer than four pentads are identified. They follow two mean paths (Fig. 8).

The first path (denoted by W_I synthesized from ten cases) is confined to the Northern Hemisphere

Table 2. *Statistics for the Independent Northward Moving TICAs*

Classification	Indian monsoon region	Western Pacific monsoon region
Number of cases (events)	13	14
Mean total northward displacement (latitude)	21	24
Mean minimum OLR ($W m^{-2}$)	−39	−39
Mean duration (pentad)	4.1	4.4
Mean propagation speed ($m s^{-1}$)	1.3	1.4

tropics and subtropics from the central or western Pacific to southeast Asia or India. Eighty percent of the events occur in June, July, and August. A typical event (Fig. 9) took place during the developing stage of the 82/83 El Niño-South Oscillation (ENSO) when the western-central Pacific is warmer than normal. A large-scale OLR low initially forms near the ITCZ in the central Pacific (150 °W, 8 °N) during August 19–23, 1982. It then migrates at an average speed of $5\,m\,s^{-1}$ across the date line and into the equatorial western Pacific in a ten-day period. By pentad 3 the OLR low deepens by $20\,W\,m^{-2}$ becoming the strongest anomaly of either sign throughout the tropics. Meanwhile, a positive OLR anomaly develops south of the Indian continent. At the fourth pentad (September 3–7), the OLR low turns west-northward extending into the South China Sea and the Indochina Peninsula. The equatorial Indian Ocean and east of New Guinea becomes dry. In the subsequent pentad, while the positive anomaly over the Indian Ocean moves to the maritime continent and merges into the dry area over the western Pacific, the TICA under consideration, however, keeps travelling northwestward, crossing the southeast flank of the Tibetan Plateau, and eventually dissipating in southeast Asia.

Another mean path (labeled as W_{II}) composed of eight cases is characterized by a cross-equatorial movement from the Southern to Northern Hemisphere in the western Pacific (Fig. 8). Figure 10 is representative of this type. The event starts with an OLR low located at 155 °W, 10 °S during the period of November 27 to December 1, 1980. The anomaly is enhanced near the date line while migrating steadily west-northwestward at a speed of about 5 degrees longitude per day. Note that the SST is warmer than normal in the western-central Pacific during the winter of 1980. It appears that this organized anomalous convection region moves across the equator in the western Pacific, and then turns northwest into the Philippine Sea, where its identity is lost.

The westward propagating events as seen from PMA OLR maps generally are significantly weaker than the eastward and independent northward moving events. The mean maximum intensity as designated by minimum OLR anomaly is -34, -39, and $-42\,W\,m^{-2}$ for westward, independent northward, and eastward moving events, respectively. Furthermore, the westward moving TICAs are smaller (usually 30–50 degrees longitude) as compared with the eastward moving ones which often have a zonal scale of 50–70 degrees longitude. In addition to weak OLR anomalies, the corresponding upward motion anomalies are also weaker. They do not always exhibit coherence with the convection anomalies. The significance of this type of low-frequency motion needs further study.

6. Geographic Dependence of the Development

The frequency of the formation and dissipation (defined as the last appearance) for the eastward moving events is presented in Fig. 11 a. The major formation region is the western central equatorial Indian Ocean, while the secondary one is the west coast of equatorial Africa. The two main dissipation regions are: the northwestern subtropical Pacific (140 °E, 25 °N) and east of the date line in the Southern Hemisphere (170 °W, 5 °S). The EE and EN modes shown in Figs. 5 a and 5 c, respectively, make major contributions to these two main dissipation regions.

Figure 11 b illustrates the geographic distribution of eastward moving events in the stage of their maximum strength. The strongest stage is most frequently observed over the eastern-central equatorial Indian Ocean. This agree with the analysis of Lau and Chan (1988). They showed that the central Indian Ocean displays strongest spectral peak with a central period of 40–50 days in OLR time series.

To reveal the preferred regions for the TICA development and dissipation, the total deepening rate of eastward moving TICAs in each $2° \times 2°$ box is shown in Fig. 12. The most favorable region for intensification is the equatorial Indian Ocean. Another minor favorable region is a broad span of the western Pacific with two centers located at 155 °E, 7 °N and 170 °W, 15 °S. These two centers are associated with the western Pacific intertropical convergence zonal (ITCZ) in boreal summer and the South Pacific convergence zone (SPCZ) in boreal winter, respectively. There are two principal regions where TICAs dissipate: the maritime continent and the equatorial region east of the date line. These statistics agree with our previous composite analysis of the evolution of the equatorial TICAs (Rui and Wang, 1989), where it was pointed out that the composite TICA rapidly in-

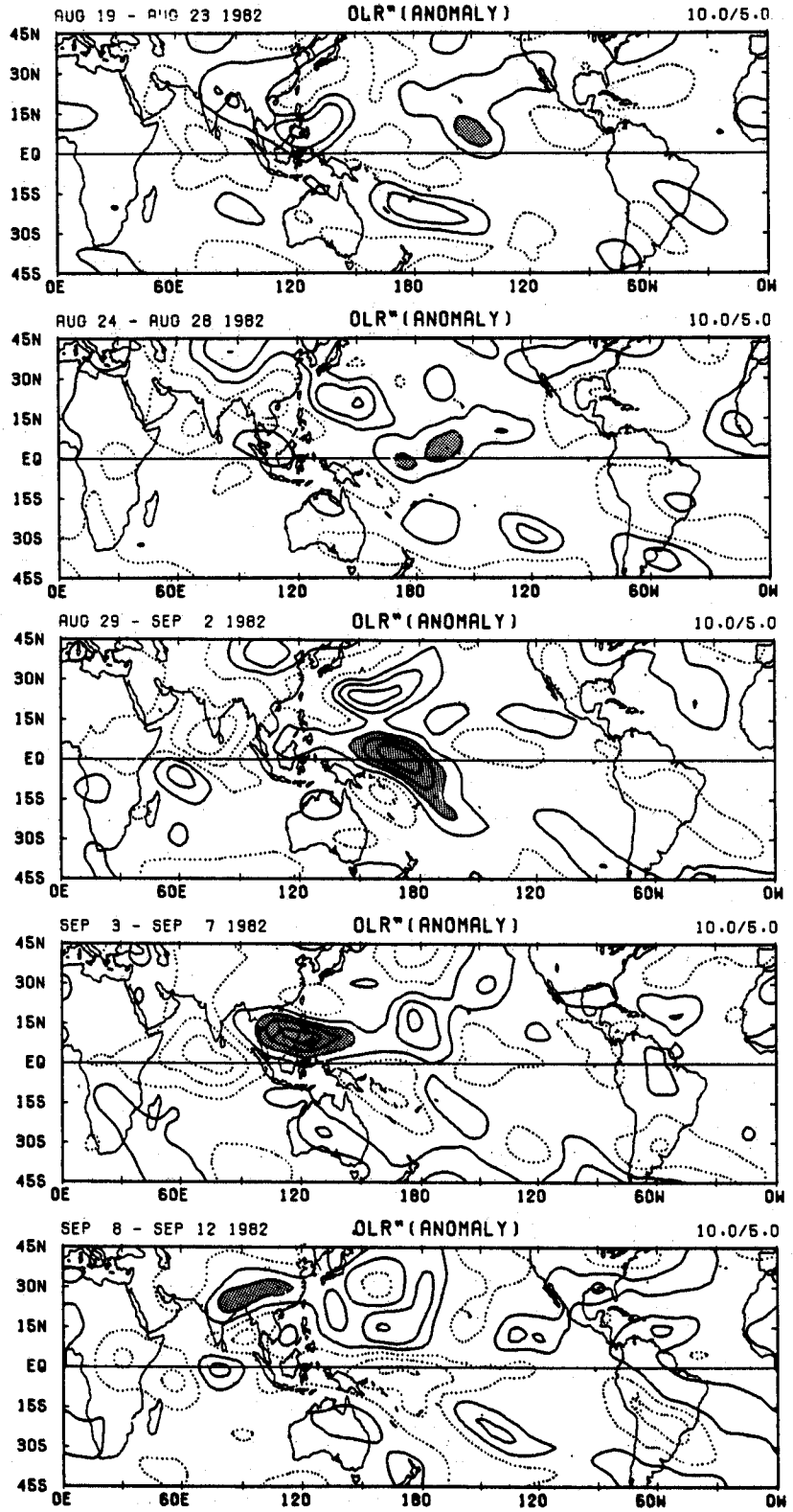

Fig. 9. As in Fig. 1 except for a Type I westward moving event occurring August to September 1982

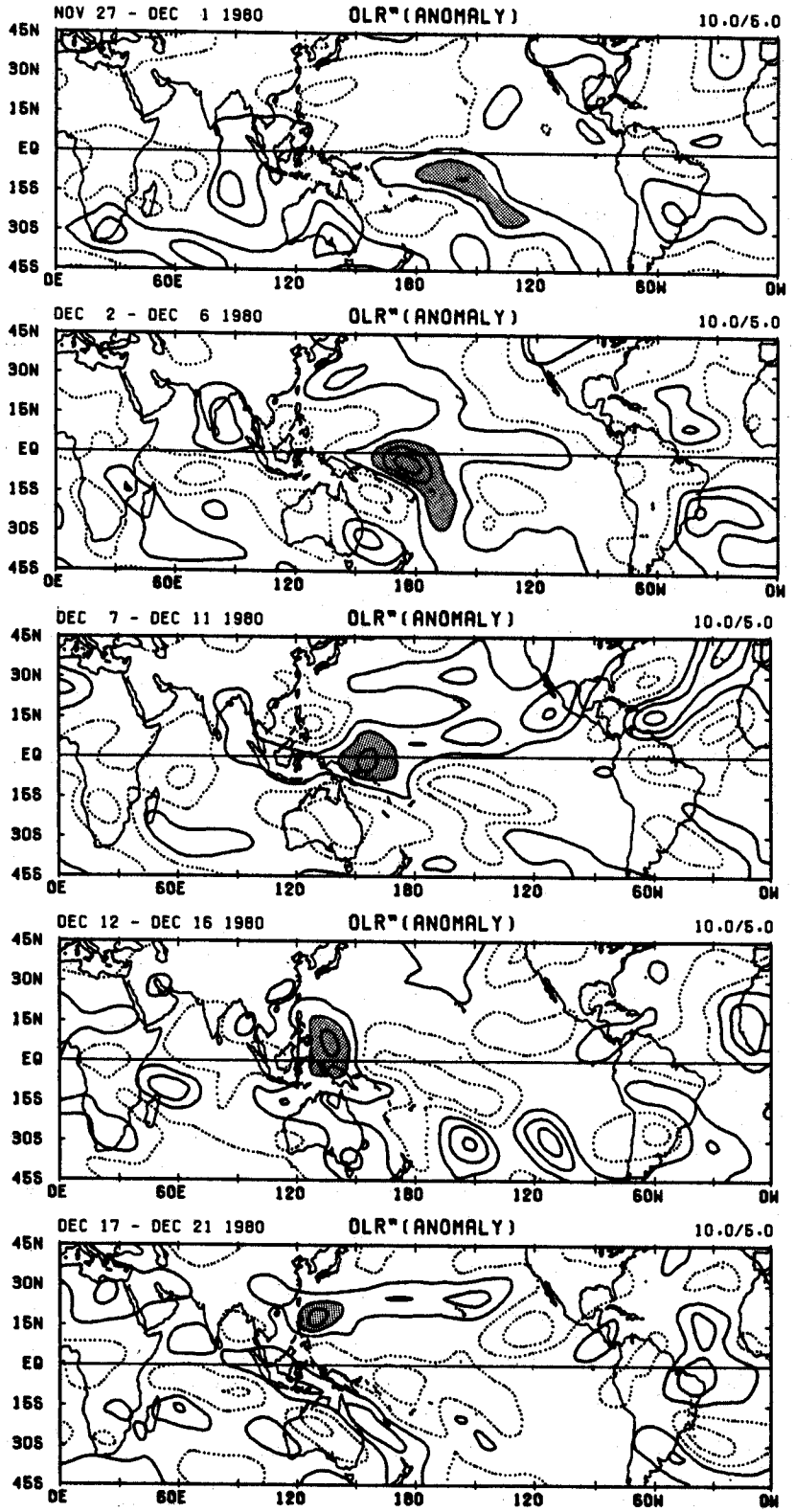

Fig. 10. As in Fig. 9 except for a Type II westward moving event occurring during November to December 1980

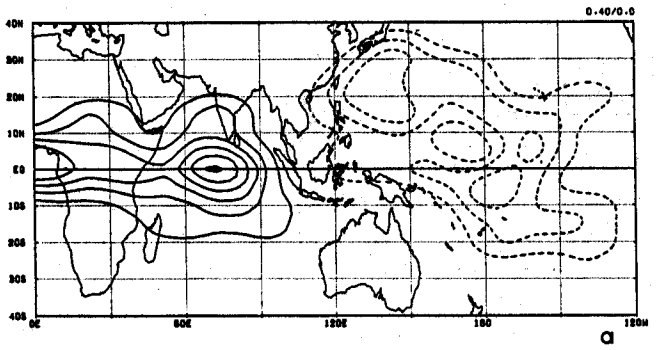

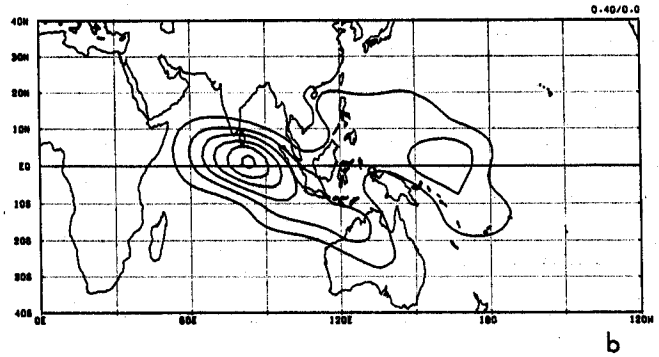

Fig. 11. Geographic distribution for the total number of (a) formations (solid contours) and terminations (dotted contours) of the eastward moving TICAs, and (b) the occurrence of the center at the strongest phase in each 2° by 2° box for the ten-year period (1975–1985). Contour interval is 0.4. Weighted smoothing has been used. The weight function is 1:2:4:2:1 in each horizontal direction

tensifies over warm water of the Indian Ocean, weakens slightly in the maritime continent, then reitensifies when passing through western Pacific, and rapidly decays after crossing the date line where sea surface temperature (SST) drops below 27.5 °C.

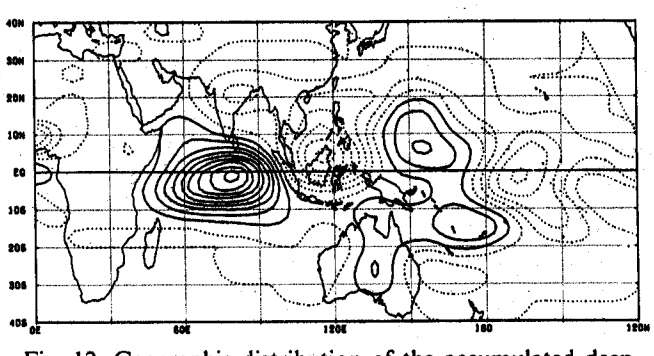

Fig. 12. Geographic distribution of the accumulated deepening rate of all eastward moving TICAs at each 2° by 2° box for ten years of period (1975–1985). Contour interval is 6 W m^{-2} pentad^{-1}. Solid (dotted) contours indicate positive (negative) value equal to or greater (less) than 3 (−3) W m^{-2} pentad^{-1}. Weighted smoothing has been used. The weight function is the same as in Fig. 11

7. Annual Variation

TICA activities exhibit significant annual variation in the frequency of occurrence for different types of events. As shown in Table 3, 78% of the equatorial eastward movement (EE mode) occurs from December to May. The occurrence of SE and NE modes is concentrated in boreal winter (November to April) and boreal summer (May or October, especially June through August), respectively. This points to a close association of the meridional component of movement with the summer monsoon circulation. The annual march of the monsoon trough and associated convergence zone appears to shift the eastward movement away from the equator over the maritime continent and western Pacific. Most EN modes take place in early and late boreal summer (May or October) but none develop during June, July,

Table 3. *Annual Variation for the Frequeny of Occurrence of TICAs.* The symbols E, N, and W denote eastward, independent northward, and westward moving events, respectively. EE, NE or SE, and EN represent three types of eastward moving modes described in Section 3. NI and NP represent independent northward moving modes over the Indian and western Pacific monsoon regions, respectively

Month		1	2	3	4	5	6	7	8	9	10	11	12	Total
E	EE	2	4	5	4	6	2	2	2	0	0	1	4	32
	SE	3	2	0	2	0	0	0	0	0	0	3	1	11
	NE	0	0	0	1	1	3	3	2	0	1	2	1	14
	EN	3	1	1	1	3	0	0	0	5	2	2	2	20
N	NI	0	0	0	0	3	2	3	1	0	4	0	1	13
	NP	0	0	0	0	3	1	5	2	2	1	0	0	14
W		0	1	0	1	1	3	4	4	0	0	2	2	18

and August. Overall, the eastward moving events occur more frequently during November through May (about 0.77 per month). In contrast, the independent northward movements over both the Indian and western Pacific monsoon region all occur in boreal summer from May to October. A similar trend, though weaker, for westward movement shows about $^2/_3$ of the events occurring in boreal summer.

The intensity of eastward-moving TICAs also displays significanct annual variation. A majority of strong events occur during boreal winter from November to April, whereas weak events most frequently occur from May to August. Thus, eastward propagation not only takes place more frequently during boreal winter, but also attains stronger intensities. On the other hand, eastward propagating events are weak in the boreal summer. One would naturally expect that stronger (weaker) intraseasonal oscillation should be observed in boreal winter (summer), if the oscillation is a statistical feature due to the dominant eastward movement of the TICAs. This indeed agrees with Madden's (1986) observational analysis. Using 19 near equator stations, he found that 40–50 day variability in zonal wind exceeds that in adjacent lower and higher frequency bands by the largest amount during December through February.

8. Summary

The 40–50 day spectral peaks found in the time series of station data in equatorial and Indian monsoon regions are believed to be caused by the systematic movement of the intraseasonal convection and circulation anomalies. Based on this hypothesis, we used pentad mean anomaly (PMA) maps to investigate climatological features of tropical intraseasonal convection anomalies (TICA).

The TICAs as seen on PMA maps normally consists of many high frequency cloud-cluster or synoptic anomalies which occur sporadically within the envelope of the large-scale OLR lows. Some of these lose their identities, while others become well-defined over adjacent regions. This process is often reflected in shape irregularities for the TICAs from one pentad to another. Although there are significant event-to-event variabilities, the continuity and persistence in their evolution, and their coherent dynamical structure between convection and circulation adds credibility to the present semi-objective analysis procedure.

One hundred and twenty-two transient TICA events were identified for ten-year period (1975–1985 with 1978 missing), among which 63% were eastward, about 22% independent northward, and 15% westward moving. All the strong events and 95% of the moderate events are moving eastward. In sharp contrast, 93% of the northward moving and 95% of the westward moving events fall in the weak category. Overall, eastward moving TICAs are definitely a dominant tropical low-frequency mode, while independent northward and westward moving TICAs are weaker modes. In addition to these transient convection anomalies, we also identified about a dozen cases of stationary events which last 4–5 pentads mainly over the central Indian Ocean region during the northern summer.

There is also a clear difference between the eastward and northward/westward propagating modes in their annual cycles. The eastward propagating mode occurs most frequently (about 72%) during December through May. This is particularly true for the strong and moderate eastward moving events – – 80% of them took place from December to May. On the other hand, all the independent northward moving TICAs occur in boreal summer from May to October, and 61% of westward moving events appear in June, July, and August.

The movement of transient TICAs as revealed in this study using event-by-event analysis displays complex patterns which augments previous findings. The eastward moving TICAs exhibit three major tracks (Fig. 5 d): (a) equatorial eastward from Africa all the way to the mid-Pacific, (b) first eastward along the equator over Africa and the Indian Ocean, then either turning northeast toward the northwest Pacific or turning southeast toward southwest Pacific at the maritime continent, and (c) eastward propagation along the equator with split center(s) moving northward in the Indian and/or western Pacific Oceans.

Independent northward propagation which is not associated with eastward propagation is found over two longitude sectors: the Indian monsoon region (70 °–90 °E, 0°–25 °N) and western Pacific monsoon region (130–150 °E, 0°–30 °N). Their existence suggests that the mechanism responsible for meridional propagation may differ from that

for the eastward propagation. This type of mode appears to be closely related to the northern summer monsoon activities.

There seem to be three dynamic and thermodynamic factors essential to the climatology of TICAs. The dominant eastward moving mode is trapped near equator. The dynamics of this mode are strongly controlled by the dynamic effect of the equator through vanishing Coriolis force and large meridional gradient of the planetary vorticity and by the thermodynamic effect of the thermal equator where SST is maximum. As Wang and Rui (1989) demonstrated in their analysis of the dynamics of the moist coupled Kelvin-Rossby wave, when the maximum SST shifts away from equator, a situation similar to that of boreal summer, the growth rate of the unstable coupled mode decreases significantly, suggesting seasonal dependence similar to the present results. Another climatological factor affecting the movement is the planetary scale monsoon and related Hadley circulations. The EN mode probably results from the influence of this background flow. The independent northward movement is possibly dominated by this effect along with the favorable SST conditions – the northward shift of the thermal equator. We are currently exploring the possible influence of environmental setting on the low frequency wave dynamics.

Acknowledgements

This research was supported by the National Science Foundation grant ATM-8814626 and the National Oceanic and Atmospheric Administration grant NA85ABH00032. The authors wish to thank Dr. T. Murakami for his OLR and ECMWF wind data, Dr. T. A. Schroeder for his comments on an early manuscript, and Mrs. D. Zee for editing the manuscript. Thanks are also extended to Mr. Z. Tang for his computational assistance.

References

Julian, P. R., Madden, R. A., 1981: Comments on a paper by T. Yasunari, A quasi-stationary appearance of 30 to 40 day period in the cloudiness fluctuation during the summer monsoon over India. *J. Meteor. Soc. Japan*, **59**, 435–437.

Krishnamurti, T. N., Subrahmanyam, D., 1982: The 30–50 day mode at 850 mb during MONEX. *J. Atmos. Sci.*, **39**, 2088–2095.

Krishnamurti, T. N., Jayakumar, P. K., Sheng, J., Surgi, N., Kumar, A., 1985: Divergent circulations on the 30–50 daytime scale. *J. Atmos. Sci.*, **42**, 364–375.

Lau, K.-M., Chan, P. H., 1985: Aspects of the 40–50 day oscillation during the northern winter as inferred from outgoing wave radiation. *Mon. Wea. Rev.*, **113**, 1889–1909.

Lau, K.-M., Chan, P. H., 1988: Intraseasonal and interannual variations of tropical convection: A possible link between the 40–50 day oscillation and ENSO? *J. Atmos. Sci.*, **45**, 506–521.

Lorenc, A. C., 1984: The evolution of planetary-sale 200 mb divergent flow during the FGGE year. *Quart. J. Roy. Meteor. Soc.*, **110**, 427–441.

Madden, R. A., 1986: Seasonal variation of the 40–50 day oscillation in the tropics. *J. Atmos. Sci.*, **43**, 3138–3158.

Madden, R. A., Julian, P. R., 1971: Detection of a 40–50 day oscillation in the zonal wind in the tropical Pacific. *J. Atmos. Sci.*, **28**, 702–708.

Madden, R. A., Julian, P. R., 1972: Description of global-scale circulation cells in the tropics with a 40–50 day period. *J. Atmos. Sci.*, **29**, 1109–1123.

Murakami, T., Nakazawa, T., 1985: Tropical 45 day oscillations during the 1979 Northern Hemisphere summer. *J. Atmos. Sci.*, **42**, 1107–1122.

Murakami, T., Chen, L.-X., Xie, A., 1986: Relationship among seasonal cycle, low-frequency oscillation, and transient disturbance as reavealed from outgoing longwave radiation data. *Mon. Wea. Rev.*, **114**, 1456–1465.

Rui, H.-L., Wang, B., 1990: Evolution characteristics and dynamic structure of tropical intraseasonal convection anomalies. *J. Atmos. Sci.*, **47**, 357–379.

Wang, B., Rui, H.-L., 1990: Dynamics of the coupled moist Kelvin-Rossby wave on an equatorial beta-plane. *J. Atmos. Sci.*, **47**, 397–413.

Weickmann, K. M., Lussky, G. R., Kutzbach, J. E., 1985: Intraseasonal (30–60) fluctuations of outgoing longwave radiation and 250 mb streamfunction during northern winter. *Mon. Wea. Rev.*, **112**, 941–964.

Weickmann, K. M., Khalsa, S. J. S., Steiner, E. J., 1990: The shift of convection from the Indian Ocean to the western Pacific Ocean during a 30–60 day oscillation. *Mon. Wea. Rev.*, **118**, 964–978.

Yasunari, T., 1979: Cloudiness fluctuation associated with the Northern Hemisphere summer monsoon. *J. Meteor. Soc. Japan.* **57**, 227–241.

Authors' address: Bin Wang and Hua Lan Rui, Department of Meteorology, University of Hawaii, Honolulu, HI 96822, U.S.A.